energies

MDPI

Review

CO_2—A Crisis or Novel Functionalization Opportunity?

Daniel Lach *, Jaroslaw Polanski and Maciej Kapkowski

Institute of Chemistry, Faculty of Science and Technology, University of Silesia, Szkolna 9, 40-006 Katowice, Poland; polanski@us.edu.pl (J.P.); maciej.kapkowski@us.edu.pl (M.K.)
* Correspondence: daniel.lach@us.edu.pl; Tel.: +48-32-259-9978

Abstract: The growing emission of carbon dioxide (CO_2), combined with its ecotoxicity, is the reason for the intensification of research on the new technology of CO_2 management. Currently, it is believed that it is not possible to eliminate whole CO_2 emissions. However, a sustainable balance sheet is possible. The solution is technologies that use carbon dioxide as a raw material. Many of these methods are based on CO_2 methanation, for example, projects such as Power-to-Gas, production of fuels, or polymers. This article presents the concept of using CO_2 as a raw material, the catalytic conversion of carbon dioxide to methane, and consideration on CO_2 methanation catalysts and their design.

Keywords: carbon dioxide (CO_2); carbon monoxide (CO); CO_2 feedstock; methanation; catalyst; catalysis; photocatalysis; Power-to-Gas; catalyst design; heterogenous catalysts database

Citation: Lach, D.; Polanski, J.; Kapkowski, M. CO_2—A Crisis or Novel Functionalization Opportunity? *Energies* **2022**, *15*, 1617. https://doi.org/10.3390/en15051617

Academic Editor: Wasim Khan

Received: 28 December 2021
Accepted: 19 February 2022
Published: 22 February 2022

1. Introduction

Life is based on carbon compounds. The dependence on coal is immanently integrated with human civilization. As the National Oceanic and Atmospheric Administration (NOAA) reports, in 2000 the annual average CO_2 concentration in the atmosphere was 369.71 ppm, in 2010 it was 390.10 ppm, and in 2020 it was 414.24 ppm [1]. The growth trend results from the increasing demand for electricity and heat. Additionally, the share of transport in the economy grows, and the current technologies in the power industry and transport are based on fossil fuels [2]. It is not quite clear whether the increase in the CO_2 atmospheric concentration of anthropogenic nature is crucial for the greenhouse effect. However, there is no doubt that phenomena related to the overloading of the atmosphere with CO_2 result in such an effect. The opinion that it is the anthropogenic CO_2 which threatens the fate of our civilization has increasingly often prevailed [3–6]. Therefore, it is very likely that this human dependence on coal leads to a critical excess of carbon dioxide in the atmosphere.

The management of CO_2 has become a key issue in the fuels and energy industry. The legislation related to this issue is the subject of European Union regulations, e.g., the European Union Emissions Trading System (EU ETS) [7] and also the Kyoto Protocol, which took effect recently [8,9]. Work related to fuel engineering and new chemistry based on carbon dioxide as the raw material has become a significant challenge. The fact that the carbon dioxide resources in the environment are becoming greater and greater is, beyond dispute, related to CO_2 ecotoxicity and its impact on climate change and the natural environment. Hence CO_2 is an easily available and cheap chemical raw material [10].

2. Carbon Dioxide Employment

2.1. CO_2 Management—Obligation and Opportunity

The first motif of CO_2 management results from the regulations, e.g., of the European Union [11]. Because a positive balance of emission is related to high financial penalties, the possibility of reducing emission is attractive in economic terms. Table 1 presents the CO_2 emission for selected economies of the European Union countries.

Table 1. Reduction of greenhouse gas and carbon dioxide emissions in selected countries of the European Union (UE). Own study based on data from [11–15].

Selected EU States	[1] GHG Emission Reduction by 2030, %	[2] GHG Emission in 2005, CO_2 Equivalent, Mt/yr	GHG Emission Limit in 2030, CO_2 Equivalent, Mt/yr	[3] Averaged Value of CO_2 Share in GHG, %	CO_2 Emission Limit in 2030, Mt/yr
Belgium	35	147.174	95.663		69.834
Luxembourg	40	13.166	7.900		5.767
Netherlands	36	225.725	144.464		105.459
Germany	38	993.712	616.101		449.754
Czech Republic	14	148.874	128.032	73	93.463
Poland	7	412.938	384.032		280.343
Slovakia	12	49.748	43.778		31.958
Lithuania	9	23.668	21.538		15.723
Latvia	6	13.081	12.296		8.976

[1] Greenhouse gases (GHG) emission reduction by 2030 as against this emission in 2005 [11]. [2] Greenhouse gases (GHG) emission in 2005 based on [12]. [3] Averaged value of CO_2 share in greenhouse gases (GHG) based on the UNFCCC (2017) [13] and IPCC (2014) [14] data.

As the most recent regulation on greenhouse gases (GHG) emission reduction [15] stipulates, the European Union member states shall reduce the GHG emission in the years 2021–2030, depending on the country, from 0 to 40% below the 2005 level. Carbon dioxide is the dominating component of greenhouse gases. Depending on the source, its share ranges between 65% and 81% [13,14]. In the near future one should expect the economy to be subordinated to the EU requirements and based on so-called smart carbon footprint management [16–21].

The second motif results from the size of the share of individual emission sources. The highest CO_2 emission is now related to the industry, namely power plants, oil and gas processing, cement production, iron and steel metallurgy, or petrochemical industry [10,22,23]. Figure 1 presents the percentage share of individual industry sectors in their total annual carbon dioxide emission.

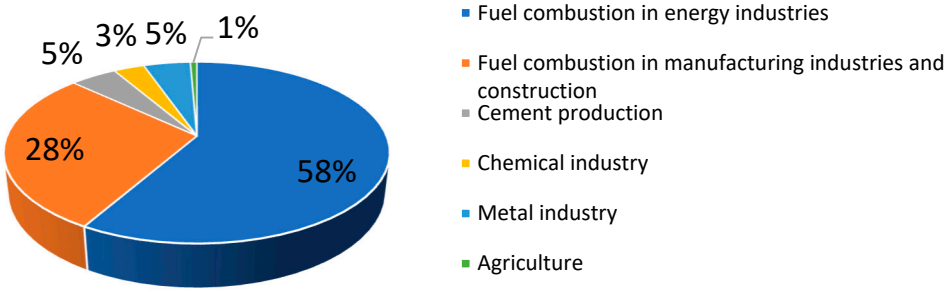

Figure 1. Percentage share of selected industry sources in their total annual CO_2 emissions in the European Union. Data for 2019, extracted from [24].

The anthropogenic impact of carbon dioxide emissions offers a great opportunity for using CO_2 as a raw material or even a feedstock wherever it is currently treated as pollutant or waste. Relatively pure carbon dioxide may be recovered from the production of hydrogen, ammonia, ethylene oxide, gas processing, natural gas liquefaction, hydrocarbons production in the Fischer-Topsch process, or biorefineries, e.g., from ethanol production [20,25]. Such technologies provide a possibility to expand simply the existing plants with units for CO_2 conversion to products useful on the chemical market. Carbon dioxide is now used in the synthesis of urea, salicylic acid, or pigments [10]. In addition, two basic product types may be distinguished, in which CO_2 plays the role of the main raw material. The first type includes inorganic or organic products, the structures of which contain the entire motif of CO_2 molecule. The second type comprises products formed in reactions, in which C-O bonds are broken. This division is of key importance in terms of energy balance and application. The first type of reaction (both inorganic and organic)

is not energy-intensive [26] and can frequently proceed spontaneously (at unfavorable kinetics), as in the production of inorganic carbonates. In the case of the second product type, the breaking of C-O bond is energy-intensive and requires the application of reducers, e.g., hydrogen. In the context of smart management of carbon dioxide balance [16–21] it is important that the energy necessary for such reaction would originate from renewable energy sources (solar, wind, geothermal, etc.) or at least from sources different than coal (e.g., nuclear energy). Otherwise, the balance of CO_2 conversion will be reduced by the amount of CO_2 emitted in the process of energy generation, used to carry out the reaction. It is also necessary to remember such factors as the blocking (storage) time of CO_2 molecules in the product. Attention was drawn to this in the report of the Intergovernmental Panel on Climate Change (IPCC) on the capture and storage of carbon dioxide [27]. A long period of use of a product formed from carbon dioxide will block CO_2 for a longer period of time, in this way preventing the reintroduction of carbon dioxide to the atmosphere. In relation to this the first type of product is more stable, e.g., inorganic and organic carbonates, and ensures long-term (from decades to centuries) immobilization of CO_2, while the second type (e.g., fuels or chemicals) immobilizes CO_2 usually for periods of months to a few years. As the second type of product over years may be subject to several cycles of processing and CO_2 releasing (depending on the product life), with the use of renewable energy sources, such technologies are at least equally as attractive as the CCS (carbon capture and storage) technologies [16].

2.2. CO_2 Processing—Examples

The annual conference, "Carbon Dioxide as Feedstock for Fuels, Chemistry and Polymers" (previously known as "CO_2 as Feedstock for Chemistry and Polymers"), in Germany is one of project sources devoted to the employment of CO_2. A few recently proposed strategies for CO_2 use, presented below, originate from there.

The Power-to-Gas (P2G) strategy [28] is a method for carbon dioxide management with good prospects. It consists in using the renewable energy or an energy surplus originating from power plants to produce chemical energy carriers. Figure 2 presents this schematically. Countries in which the power industry is to a large extent based on renewable energy sources (e.g., wind or solar) encounter problems with the energy surplus storage or management [28]. According to the P2G strategy this problem may be resolved by the use of this surplus for water electrolysis, resulting in the origination of hydrogen, which in turn in a reaction with carbon dioxide forms methane or methanol, which are compounds which may be stored and used as an energy source in industry and in the power sector [29,30]. Such processes still require optimizing, increasing the overall productivity, and minimizing the costs. Nevertheless, since 2011 we have been observing a growth of such projects in countries like Germany, Denmark, Switzerland, or Spain [28].

The utilization of CO_2 to produce polymers and chemical compounds is another opportunity for its use [31]. In this way, for example, polyhydroxy alcohols (polyols), polypropylene carbonate (PPC), and cyclic carbonates are obtained. Propylene carbonate and ethylene carbonate is mainly synthesized by catalytic CO_2 cyclization to epoxides [32]. The use of non-toxic and freely available CO_2 not only allows the achievement of compounds with higher added value, but also makes the reaction an example of a green process. Moreover, the reaction is thermodynamically favorable as it uses the high free energy of the epoxides to balance the high thermodynamic stability of the carbon dioxide. However, the differentiation in the rate of the CO_2 cycloaddition reaction depending on the starting substrates, and thus competition with the reaction yielding polycarbonate by-products, requires selective catalysts. Active sites on the catalyst surface are Lewis acids. Therefore, Kelly et al. grafted $ZrCl_4 \cdot (OEt_2)_2$ on the surface of dehydroxylated silica at 700 °C (SiO_2-700) and 200 °C (SiO_2-200) by surface organometal chemistry (SOMC), and tested in the cycloaddition of CO_2 (also from CO_2 from cement factory flue gas) with propylene oxide [33]. As reported by the authors, despite a certain degree of leaching of weakly bound or absorbed zirconium complexes during the first catalysis, the catalyst was active, recov-

erable, and suitable for reuse in further catalytic cycles. Then, Sodpiban et al. described the heterogeneous catalysts consisting of metal halides ($ZnCl_2$, $SnCl_4$) as active precursors immobilized on the surface silica with ionic liquids that were based on functionalized quaternary ammonium halide salts [34]. The best catalytic systems ($ZnCl_2$(1.99)-IL-I and $SnCl_4$(0.66)-IL-Br) allowed for the practically quantitative conversion of terminal epoxides to the corresponding carbonates under relatively mild conditions (25–40 °C, 1 bar). The catalysts were also tested in a stream of dilute gases of CO_2 (50% CO_2/N_2 mixture) and CO_2 from contaminated sources (20% CH_4 in CO_2 with H_2S as the catalyst poison), obtaining quantitative conversion for the above-described catalysts. The catalysts were deactivated only by the loss of the silica matrix and dehalogenation of quaternary ammonium halide groups with simultaneous poisoning of the active metal centers. Metal-organic frameworks (MOFs) or porous organic polymers (POPs) are new trends in the search for CO_2 cycloaddition catalysts [32]. MOFs are porous crystalline materials with a defined structure and high development of the specific surface area—SSA. On the other hand, POP can be an ideal structure for porphyrin metal (Mg or Al) complexes, giving highly active and selective catalysts under mild conditions [35]. The research carried out in this area allows us to render the financial benefits on market principles. For example, there are already commercial plants producing ethylene carbonate in the reaction of epoxide with carbon dioxide (Asahi Kasei Corporation, Japan). In turn, Novomer, Bayer, or BASF are carrying out investments aimed at implementation of such projects. Breakthrough innovations are expected there [36]. For example, polypropylene carbonate produced with the use of carbon dioxide contains 43 wt% of CO_2. It is biodegradable, stable at high temperatures, flexible, transparent, and features a shape memory effect. This interesting profile of practical properties translates into a wide range of applications. PPC is used in production of packaging foils; foams; softeners; and dispersants for brittle plastics, in particular for originally brittle bioplastics, e.g., polylactic acids (PLA) or polyhydroxyalkanoates (PHA). PPC is frequently used in the production of new materials. PPC combination with PLA or PHA results in obtaining biodegradable, semi-transparent, and easy to process plastics, replacing the widely used acrylonitrile butadiene styrene (ABS). Polyethylene carbonate (PEC) is an equally often studied polymer which employs CO_2. PEC is used as a substitute or additive to traditional plastics made from petroleum. PEC contains 50 wt% of CO_2. Its most interesting practical property consists in the resistance to oxygen transport (permeation), which makes it an interesting packaging material for food. Polyurethane blocks made from polyols, obtained from carbon dioxide, are another example. Such products are used as mattress foams and insulating materials.

Another idea consists in the use of CO_2 as a source of carbon for industrial biotechnologies. In this strategy carbon dioxide is used as food for algae or bacteria [37–40]. In the first case CO_2 feeds cultures of microalgae in special photo-bioreactors or in open ponds. In this case algae may be genetically modified to increase its effectiveness. Biomass is the end product. This method is willingly used to produce various chemicals, in particular in the production of biodiesel and aircraft fuel. The second strategy assumes the use of genetically modified bacteria, which use CO_2 as a source of metabolic carbon, and at the same time as the skeleton to produce specially designed molecules. Modern biotechnology offers already a possibility to "reprogram" bacteria towards synthesis of specified targets. Intensive work continues on modern bacteria strains capable of carbon dioxide consumption and its conversion into specified chemical products [39,40]. An interesting example is the recent research on carbonic anhydrases (CA), enzymes found in algae, archaea, eubacteria, vertebrates, and plants that can convert CO_2 into bicarbonate ions [41]. CA catalyzes the hydration of CO_2, which can finally lead to $CaCO_3$ in the presence of Ca^{2+}. In turn, $CaCO_3$ is already a raw material, e.g., for cement or ceramics. The main advantages of CA include the economically viable sequestration of carbon dioxide and its carbonation at low concentration. However, despite the high catalysis rate, the stability of CA is a significant challenge for its industrial applications. However, these difficulties have been partially

overcome by strapping CA on appropriate surfaces, e.g., biochar, alginate, polyurethane foam, or nanostructured materials.

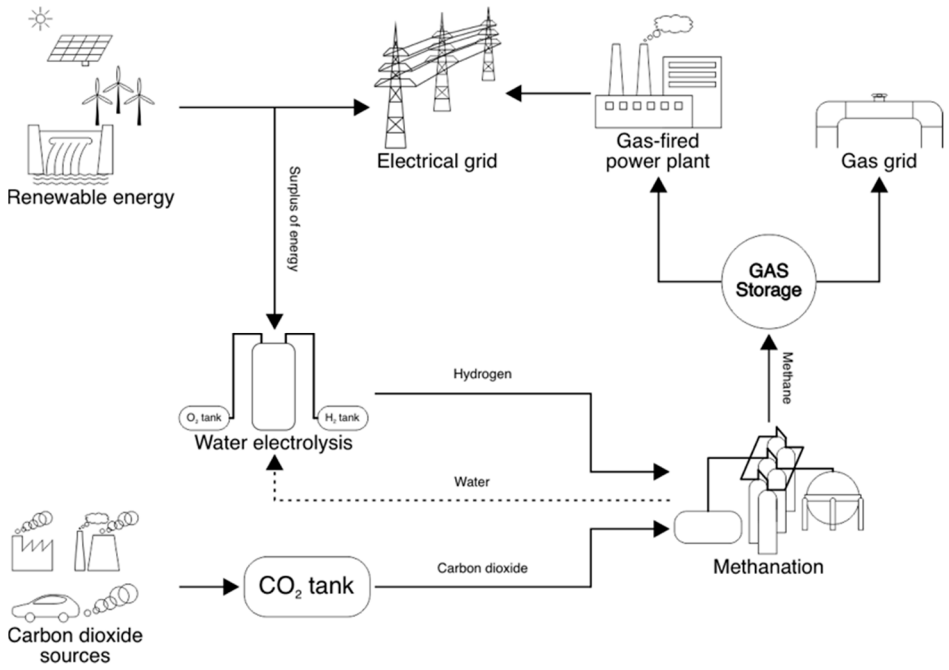

Figure 2. Power-to-Gas strategy. Energy from renewable energy sources is used in electrolysis to produce hydrogen. Hydrogen with carbon dioxide is converted into methane in the CO_2 methanation process. The methane is then stored, released into the gas grid, or used in cogeneration and in gas turbines to produce energy.

Preparing an environmentally friendly solvent and agent with specific properties can also involve carbon dioxide. The subject matter is a supercritical fluid of CO_2 [42]. Such a fluid behaves like gas and liquid at the same time. It is gas-like because it is inviscid and expands to fill a container and liquid-like in terms of density, high heat capacity and conductivity, and solubility. It is non-toxic, non-explosive, thermally stable, and widely available. It is mainly used as a solvent or working fluid. Supercritical CO_2 is an effective solvent for complicated extractions, e.g., nonpolar organic compounds. It does not cause the toxic residual solvent problem, and it is easy to separate/remove from the system. Due to its low critical point, it is an ideal liquid for extracting volatile compounds, compounds with high molecular weight, and compounds with a low degradation temperature. Supercritical CO_2 has proved helpful in the following areas:

- in pharmacy to reduce the particle size of a drug, improving its solubility, and thus bioavailability [43–47],
- in impregnating the compound in pre-formed carrier particles, e.g., of the active compound on the drug carrier [48],
- in micronization and creation of nanoparticles [44,47], and in the development of environmentally friendly dyes [49] and DSSCs (dye-sensitized solar cells) technology [50],
- as an advantage over conventional extraction of, e.g., essential oils from herbs that exhibit various biological, therapeutic, and aromatic properties [51,52].

The critical temperature and pressure of carbon dioxide (Tcr = 31.1 °C and $p$cr = 73.8 bar) are roughly similar to the ambient conditions. Supercritical CO_2 reduces the compression work significantly in the closed-loop compression cycle. Heat dissipation to approximately ambient temperature is observed. Therefore, it is also an attractive working fluid in energy generation technologies and systems, as amply summarized in [53].

However, the use of carbon dioxide would not be possible without an appropriate method of its capture. The equipment of Climeworks company offers an interesting

solution [54], which sucks the air containing CO_2 or exhaust gas, and with the involvement of special filters made of porous granulate modified with amines, binds CO_2. After the filter saturation with carbon dioxide it is heated to approx. 100 °C, using low-quality heat as the source of energy. CO_2 is released from the filter and gathered in the form of pure gas, which may be used as a substrate. The air free of carbon dioxide is released into the atmosphere. The cycle is repeated and the applied filters may be used many times, even in a few thousand cycles. This technology may be an important element in the aforementioned concepts, but it is important first of all as an industrial "generator" of clean air. Moreover, the topic of separating CO_2 from gases is being intensively developed even with computational modeling. For example, Ghiasi et al. report that the calculated permeation barrier, selectivity, and thermodynamic functions for CH_4, H_2S, N_2, and CO_2 passing through finite porosity graphene doped with nitrogen atoms indicate a highly efficient and selective material for carbon dioxide separation [55]. In turn, Shaikh et al. describe the reaction mechanism of CO_2 absorption by the amino-acid ionic liquid [56]. They reveal the reaction pathway employing DFT calculations. Using the MD method, they report the cation–anion interaction for two different glycinate-based ionic liquids with structurally similar cations with different alkyl chain lengths. Since the gases for CO_2 recovery are approximately 10% water, the authors also provide simulations with its participation. They note that the interaction between the cation and anion is reduced in the presence of water by reducing the diffusion coefficient of the cation, thus reducing carbon dioxide uptake. Nevertheless, ionic liquid is a promising agent for CO_2 capture, due to the high CO_2 solubility, recycling (almost zero vapor pressure), and fine-tuning dependence on the task.

3. Carbon Dioxide Methanation and Nanocatalysis—The Focal Point in CO_2 Conversion

Catalysis is one of important elements of smart CO_2 management. In particular, many papers have been devoted to catalytic conversion of carbon dioxide to methane. Figure 3 shows an increasing number of papers.

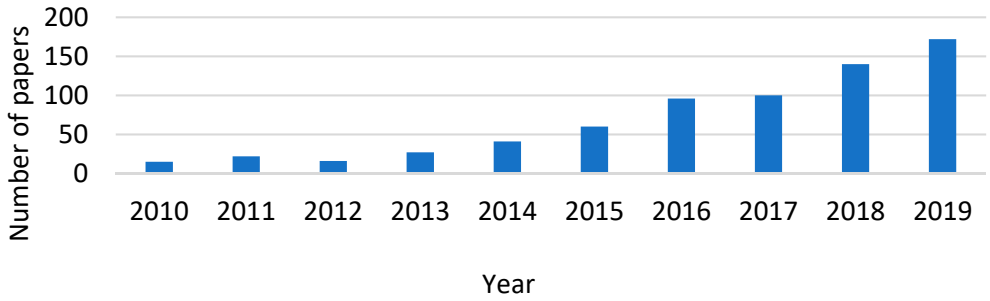

Figure 3. Quantity of publications on catalytic CO_2 methanation from 2010 to 2019. Data from the ISI Web of Science (Thomason Reuters) database. Query conducted for: "catalytic CO_2 methanation".

Catalytic methanation is a central issue of the Power-to-Gas concept [28]. According to statistics, in 2011 the share of papers on CO_2 methanation in all Power-to-X projects (where X is: Gas, Power, Chemicals) was already 27% (Figure 4). The share of catalysis among various CO_2 methanation strategies was 44% and that was the second largest contribution, immediately next to biological methods.

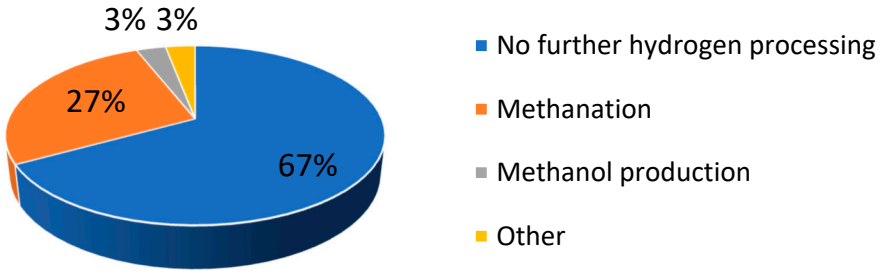

Figure 4. Share of further processing of hydrogen in Power-to-X (X: Gas, Power, Chemicals, Fuels). Data extracted from [28].

3.1. CO_2 Methanation

Carbon dioxide hydrogenation was considered for the first time by Paul Sabatier and Jean B. Senderens in 1902. In the paper "Nouvelles syntheses du methane" [57] they proved that one mole of methane may be obtained in the reaction of one mole of carbon dioxide with four moles of hydrogen, acc. to reaction:

$$CO_2 + 4H_2 \rightleftarrows CH_4 + 2H_2O$$

This reaction is exothermic and spontaneous. At room temperature (~25 °C) its enthalpy (ΔH) is −165 kJ/mol and the Gibbs free energy (ΔG) is −113.5 kJ/mol [10]. ΔG describes the maximum free energy (energy that can be turned into work) that can be released or adsorbed when it goes from the initial state to the final state. In the CO_2 methanation, a negative ΔG indicates that the substrates (initial state) have more free energy than the products (final state). Therefore, the move towards products involves the release of energy. Energy does not have to be provided for the reaction to occur—it occurs spontaneously. In turn, ΔH refers to the difference between the bond energy of products and substrates. A negative ΔH means a heat release during the reaction towards the products. In the temperature range from 25 to 500 °C, ΔG and ΔH is presented in Figure 5. If the reaction is exo-energetic in one direction, it is also endo-energetic in the opposite direction. Therefore, if the Gibbs free energy in methanation increases rapidly with the rise of temperature (provision of thermal energy), so that above 500 °C it becomes positive, then in the high temperature range, the reverse reaction—methane reforming ($CH_4 + H_2O \rightleftarrows CO + 3H_2$)—prevails and disturbs the obtaining of methane [58]. However, the course of CO_2 methanation is more complicated and may comprise many intermediate or side reactions. Jiajian Gao specifies them in Table 2 and gives their equilibrium constant K from 200 to 800 °C in Figure 6 [59].

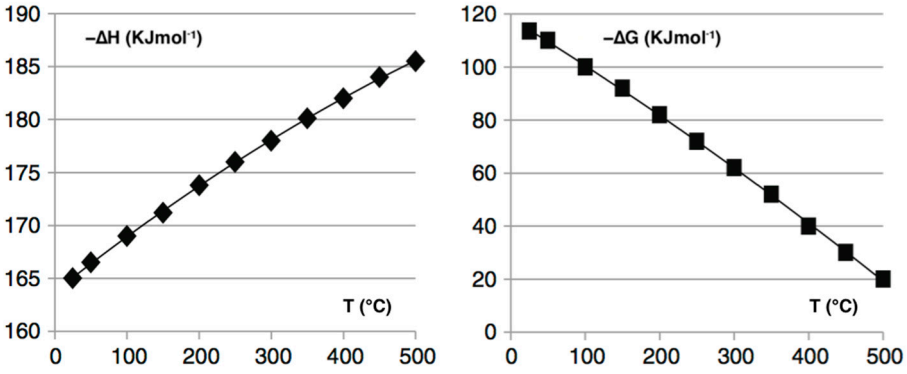

Figure 5. Enthalpy and Gibbs free energy for CO_2 methanation in the temperature range from 25 to 500 °C. Data extracted from [10].

Table 2. Main possible reactions during carbon dioxide methanation. Data extracted from [59].

Reaction Number	Reaction Equation	$\Delta H_{298\ K}$, kJ mol^{-1}	$\Delta G_{298\ K}$, kJ mol^{-1}
R1	$CO + 3H_2 \Longleftrightarrow CH_4 + H_2O$	−206.1	−141.8
R2	$CO_2 + 4H_2 \Longleftrightarrow CH_4 + 2H_2O$	−165.0	−113.2
R3	$2CO + 2H_2 \Longleftrightarrow CH_4 + CO_2$	−247.3	−170.4
R4	$2CO \Longleftrightarrow C + CO_2$	−172.4	−119.7
R5	$CO + H_2O \Longleftrightarrow CO_2 + H_2$	−41.2	−28.6
R6	$2H_2 + C \Longleftrightarrow CH_4$	−74.8	−50.7
R7	$CO + H_2 \Longleftrightarrow C + H_2O$	−131.3	−91.1
R8	$CO_2 + 2H_2 \Longleftrightarrow C + 2H_2O$	−90.1	−62.5

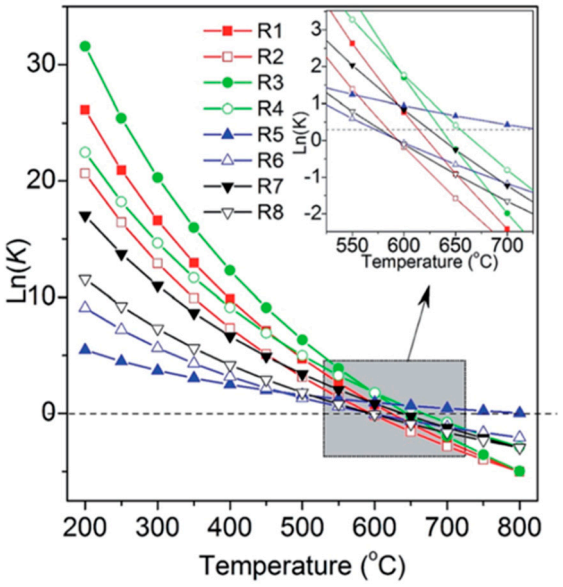

Figure 6. The equilibrium constants (K) for the reactions presented in Table 2, in the temperature range from 200 to 800 °C. © Adopted from [59].

Analysis of the above data can conclude that the temperature is the main parameter affecting the equilibrium. Therefore, from the thermodynamic point of view, the methanation reaction of carbon dioxide should be carried out at low temperatures. However, under such conditions the reaction rate goes down. Hence the CO_2 hydrogenation requires the application of a catalyst [23,60]. It allows the achievement of an acceptable reaction rate and a reduction in the cost of the process itself [61,62].

3.2. Catalyst in Methanation

Metals from group VIII to XI stand out among methanation catalysts [63]. Nickel is probably the most frequently studied metal [64–67]. It features the most favorable ratio of metal price to its activity. Additionally, ruthenium and rhodium show interesting properties [67–71]. In the case of Ru and Rh catalysts, apart from a high activity, their ability to prevent sintering and accumulation of carbon particles is their important advantage, which makes them additionally resistant to deactivation. In addition, Ru stands out in the low-temperature methanation, e.g., in the Ru/TiO_2 system [72] or Ru/Ni_nanowires [73]. A low temperature is an important parameter optimizing the thermodynamic and energy efficiency. Numerous studies are related to the possibility of lowering the temperature. Using the example of selective carbon monoxide (CO) methanation [74], Table 3 presents a summary of studies in this field.

Table 3. Profile of selected catalysts in CO methanation. Data extracted from [74].

Catalyst	[1] WHSV, $cm^3\ g^{-1}\ h^{-1}$	[2] GHSV, h^{-1}	Composition of Inlet Gases, %	[3] Reaction Characteristic and Yield				
			$CO/CO_2/H_2O/H_2$	T_{min}, °C	S_{min}, %	T_{max}, °C	S_{max}, %	mol CO $g^{-1}\ h^{-1}$
10% *w*/*w* Ni/CeO_2	26,000	46,000	1.5/20/10/60	250	89	320	50	0.0160
			1/20/10/60	240	100	315	45	0.0106
			0.5/20/10/60	230	99	290	31	0.0053
	6000	12,000	1/20/10/60	210	100	265	50	0.0025
	13,000	26,000		225	100	280	50	0.0053
	43,000	84,000		265	94	295	54	0.0176
10% *w*/*w* Ni/ZrO_2	~150,000	-	0.5/14.8/0.8/59.2	280	~90	300	~70	0.0307
1.6% *w*/*w* Ni/ZrO_2	-	10,000	1.14/21.43/1.8/74.8	260	~60	280	~60	-
10% *w*/*w* Ni/TiO_2	-	10,000	0.2/16.1/18.4/65.3	200	~80	-	-	-
5% *w*/*w* Ru/TiO_2	~150,000	-	0.5/14.8/0.8/59.2	220	~70	260	~20	0.0307
5% *w*/*w* Ru/TiO_2	27,000	-	0.5/18/15/40	220	60	260	20	0.0055
5% *w*/*w* Ru/ZrO_2				265	80	310	50	0.0055
5% *w*/*w* Ru/CeO_2				250	75	300	30	0.0055
3% *w*/*w* Ru/Al_2O_3	-	13,500	0.9/24.5/5.7/68.9	220	<50	-	-	-
2% *w*/*w* Ru/Al_2O_3	-	10,000	0.3/4.8/75/18.8	270	<20	-	-	-
30% *w*/*w* Ru/CNT	12,000	-	1.2/20/0/78.8	220	-	-	-	0.0059
30% *w*/*w* Ru-ZrO_2/CNT				180	100	240	35	0.0059
1% *w*/*w* Ru/MA-33Ni	-	2800	0.9/17/15/67.1	185	100	245	50	-
1% *w*/*w* Ru/MA-40Ni	-			185	100	260	50	-
1% *w*/*w* Ru/MA-50Ni	-			195	100	270	50	-

[1] WHSV—weight hourly space velocity (flow of reagents per unit of catalyst mass in the unit of time). [2] GHSV—gas hourly space velocity (volumetric flow of reagents per unit of catalyst volume in the unit of time). [3] T_{min} and T_{max}—minimum and maximum temperature, setting the range in which CO concentration in the reformate is less than 10, or 20 ppm in a few cases. S_{min} and S_{max}—reaction selectivity at T_{min} and T_{max}, respectively.

Another issue is the catalyst activity dependence on the support, on which the selected metal has been placed. For the catalyzed reaction it is favorable to maximize the metal surface area for a specific metal weight [75]. Therefore, small metal particles are synthesized (usually smaller than 1–10 nm), with a narrow size distribution, but with a uniform location on a large specific surface of a thermally stable substrate [23,63,76]. Hence, support in the form of oxides (e.g., SiO_2, Al_2O_3, TiO_2), zeolites, carbon, or metaloorganic compounds is distinguished. Support affects also the adsorption and catalytic properties. Figure 7 may be an example, presenting the difference between the selected oxide support of nickel catalyst and the yield of CO_2 methanation.

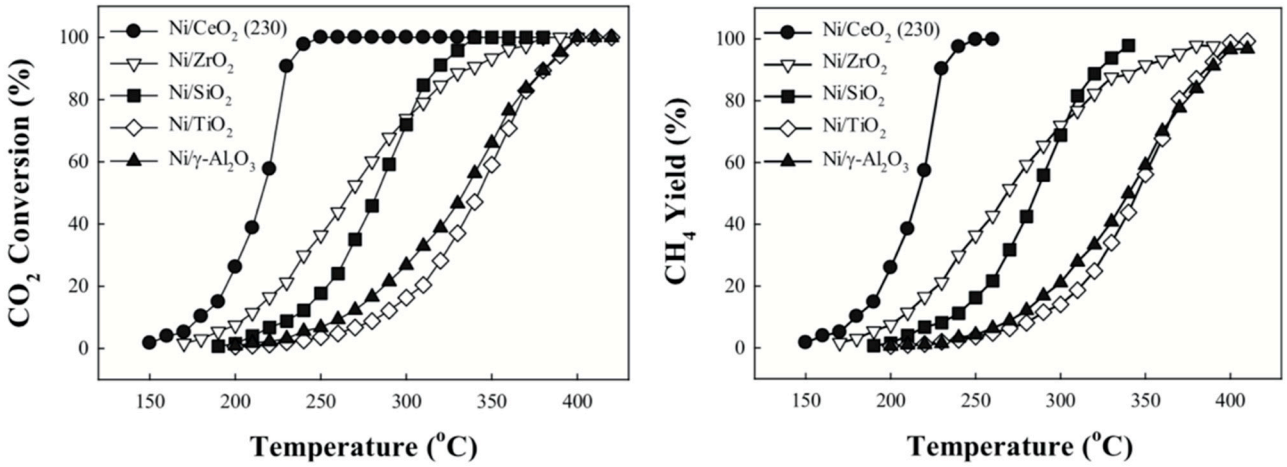

Figure 7. Impact of catalyst supports on the yield of CO_2 to CH_4 conversion. Reaction conditions: 1 mol% CO_2, 50 mol% H_2, 49 mol% He, F/W = 1000 mL/min/g_{cat}. © Adopted from [77].

Studies on the support of methanation catalyst were enhanced with studies on catalytic promoters, that is, substances added to improve or change the catalyst operation. MgO is an example of a catalyst promoter which, introduced to Ni/Al_2O_3 catalyst, increases the thermal stability [78] and resistance to carbon parts precipitation [79]. La_2O_3 increases the Ni/Al_2O_3 catalyst activity via the increase in the nickel dispersion and hydrogen capture [80]. The enhancement of nickel catalyst with V_2O_3 improves its activity, thermal stability, and resistance to sintering [81]. The addition of CeO_2 allows the achievement of a higher susceptibility to reduction and long-term stability [82]. In turn, potassium increases the selectivity towards conversion to higher hydrocarbons [83]. In the context of obtaining methane this is obviously not a desired effect.

The type of support is significant for the CO_2 methanation mechanism [71,84–87]. Hydrogenation of carbon dioxide may proceed via various paths through different structures, which include CO, -OCH_3, and $HCOO^-$ groups. Their origination, further reaction, as well as adsorption and desorption frequently depend on the morphology of the support surface. For example, mezostructural silica, which due to the presence of internal and interparticle pores increases the number of free oxygen sites in the catalyst, is decisive in a particular mechanism of the reaction [88–90]. It is schematically presented in Figure 8. According to this theory, CO_2 and H_2 are adsorbed on the metallic catalyst. As a result of the dissociation of molecular forms, CO, O, and H originate then, which can migrate to the carrier surface. In the next stage CO reacts with oxygen from the carrier surface, forming formate or carbonyl groups in a bridge or bidentate system. In addition, the formation of bidentate formate requires an additional reaction with hydrogen. An oxygen atom is subject to surface stabilization through interaction with electron gaps of the oxide carrier, close to the metal. Oxygen stabilized in this way reacts with hydrogen forming a hydroxyl group, which in a further reaction with hydrogen will form a molecule of water. Oxygen-rich forms of carbon formed on the surface, that is, carbonyl and formate, are hydrogenated to methane.

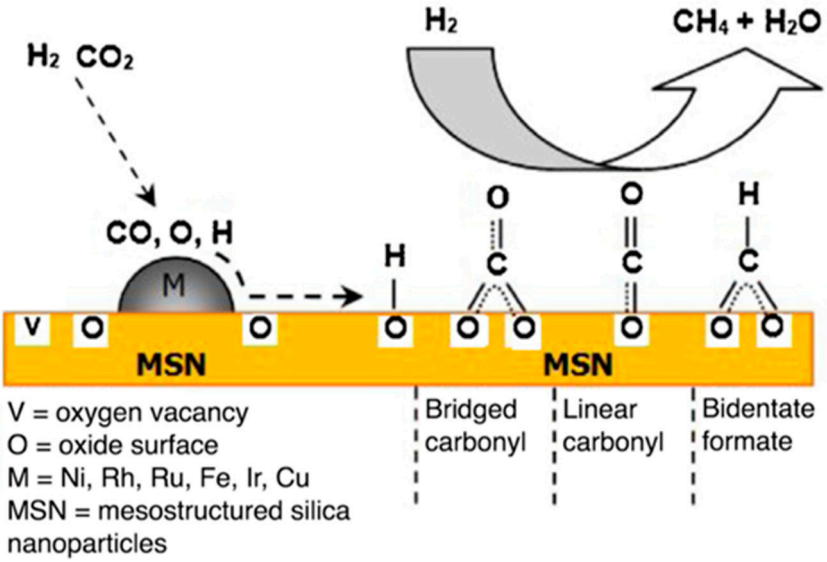

Figure 8. Likely mechanism of CO_2 methanation using the catalyst that is based on mesostructured nanosilica support. © Adopted from [88].

The subsequent essence of matters is the diffusion effect [91,92]. It is a process on the catalyst site that, in a simplified description, may include the following steps: (1) transport of the reactants from the gas phase to the catalyst surface (external diffusion), (2) diffusion of substrates to the surface inside the catalyst pores (internal diffusion), (3) surface operations (chemisorption and catalytic reaction), (4) diffusion of reaction products from inside the catalyst pores to the outside surface (internal diffusion), and (5) migration of reaction products from the catalyst surface to the gas phase (external diffusion). Depending on the morphology of the catalytic surface, the effect of external and internal diffusion is considered. The external diffusion effect depends on the size of the catalyst grains, the flow rate, and the diffusion properties of the reactants. In turn, the internal diffusion effect depends on the porosity of the material, the pore size and distribution, pore connectivity, and the size of the catalytic material grains. The diffusion effect is even more significant when considering the concentration and temperature gradients inside and over the catalyst surface. This topic is discussed in detail in the review [93]. Nevertheless, it is worth noting that this effect is often wrongly ignored, which causes a misinterpretation of the results. Diffusion plays a role in such essential factors as the rate and bottleneck of the reaction or the conversion and product distribution.

The combination of metal and specified support is also frequently studied in the photocatalytic methanation [94]. It was observed that the application of heat and light together can minimize the energy consumption and ensure unique features which cannot be achieved in conventional thermocatalytic reactions [95–97]. Light absorbed by metallic nanoparticles of the catalyst and by reagents existing on their surface is a source of intraband or interband transformations, which generate electrons with a high kinetic energy, so-called hot electrons [97–99]. Hot electrons are effective activators of reagents or intermediate compounds. As a result, a reduced activation energy is observed [100]. For example, in the reaction of carbon dioxide methanation, at 150 °C, hot electrons formed as a result of light absorption by a CO_2 molecule (adsorbed on the metallic surface of Ru/SiO_2 catalyst) increase the conversion of carbon dioxide to methane from 1.6% to 32.6% [101]. Figures 9 and 10 compare Ru/SiO_2 and Rh/SiO_2 catalysts in the CO_2 methanation with the involvement of light and without.

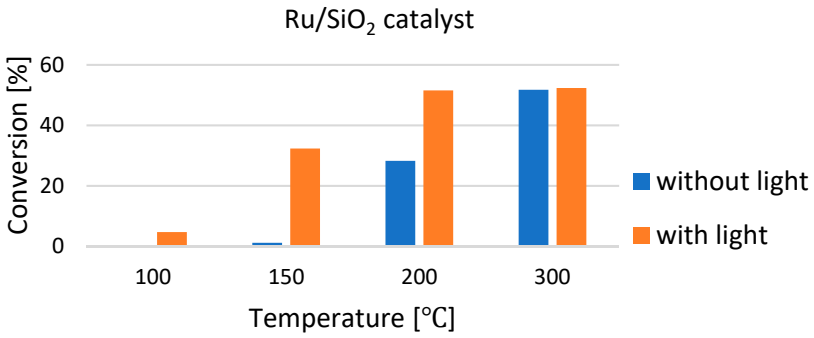

Figure 9. CO_2 conversion on Ru/SiO_2 catalyst with and without light. Data extracted from [101]. Conditions: 0.5% vol. CO_2/N_2 (50 sccm) and H_2 (1.5 sccm). Lamp parameters: Xe 35 mW cm^{-2} with water cooling to exclude the heat effect from the light.

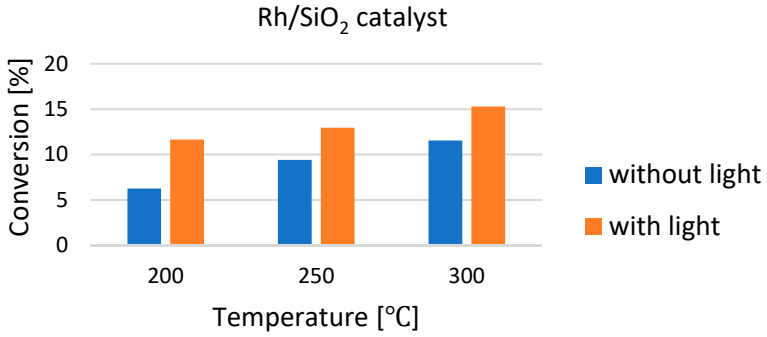

Figure 10. CO_2 conversion on Rh/SiO_2 catalyst with and without light. Data extracted from [101]. Conditions: 0.5% vol. CO_2/N_2 (50 sccm) and H_2 (1.5 sccm). Lamp parameters: Xe 35 mW cm^{-2} with water cooling to exclude the heat effect from the light.

The activity of these catalysts is additionally conditioned by the size of metal nanoparticles (Figure 11). Larger nanoparticles, e.g., ≥5 nm, reduce the activation barrier for CO_2 molecule dissociation on the metal surface. In the case of a photosensitive system this results in a larger number of hot electrons, which improve the reaction kinetics.

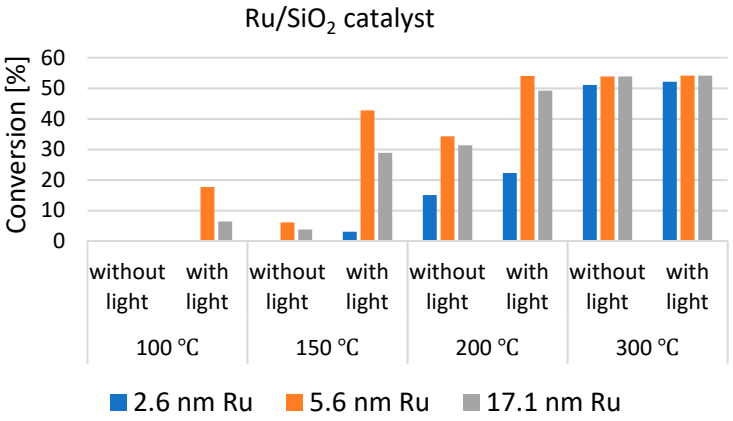

Figure 11. CO_2 conversion on Ru/SiO_2 for different sizes of Ru nanoparticles. Data extracted from [101].

The last issue is the method of catalyst preparation. The selection of preparative method may determine such factors as the size and shape of metal nanoparticles, their uniform distribution on the support, limitation of nanoparticle aggregation, as well as minimization of the used metal [75,102]. Many various methods have been presented in the review entitled "Methods for Preparation of Catalytic Materials" [102]. However, in the context of the aforementioned silica becoming increasingly popular in nanomethods,

a proprietary method of our team may draw attention. The method comprises two main stages. The first of them consists in the synthesis of amorphous silica, which plays the role of an intermediate carrier and matrix for metallic nanoparticle generation. The second is the matrix digesting and transferring nanoparticles of the selected metal onto the target support. It is graphically presented in Figure 12. Silica is synthesized by the Stöber method [103]. The aim consists in obtaining spherical, monodisperse, and uniform sizes of silica nanoparticles from the water solution of alcohol and silicon alcoxides at the presence of ammonia as the catalyst. Two basic reactions are distinguished:

$$\text{Hydrolysis: Si-(OR)}_4 + \text{H}_2\text{O} \rightleftarrows \text{Si-(OH)}_4 + \text{4R-OH}$$

$$\text{Condensation: 2Si-(OH)}_4 \rightleftarrows \text{2(Si-O-Si)} + 4\text{H}_2\text{O}$$

Hydrolysis leads to the formation of silanol groups, while siloxane bridges result from the condensation polymerization. The reaction product depends on the type of silicon alcoxide and alcohol. The authors of the methods emphasize that particles prepared in solutions are the smallest, and the particle size increases with the growing length of the alcohol carbon chain. Rao et al. [104] in turn pay attention to the size and deviation of silica grain size through modification of the concentration of silicon alcoxide and alcohol, ammonia concentration, water content, and the change of reaction temperature. This allows the fine-tuning of the physical properties of silica, which is extremely important for later generation of specified sizes of metal nanoparticles. The second stage comprises nanometal growing on the matrix, reducing the intermediate conjugate (metal-silica) with hydrogen, digesting the silica with lye (when other support is needed), transferring metallic nanoparticles onto the surface of the target support, or separating metal nanoparticles. This method allows for nanomanipulation of nanoparticles' size and shape, reduction of their tendency to aggregate and form lumps, and for reduction of the amount of used material. So far this method has worked well in preparing high-performance catalysts for ammonia cracking [105], CO_2 methanation [73,106,107], glycerol oxidation [108], and Sonogashira coupling [109].

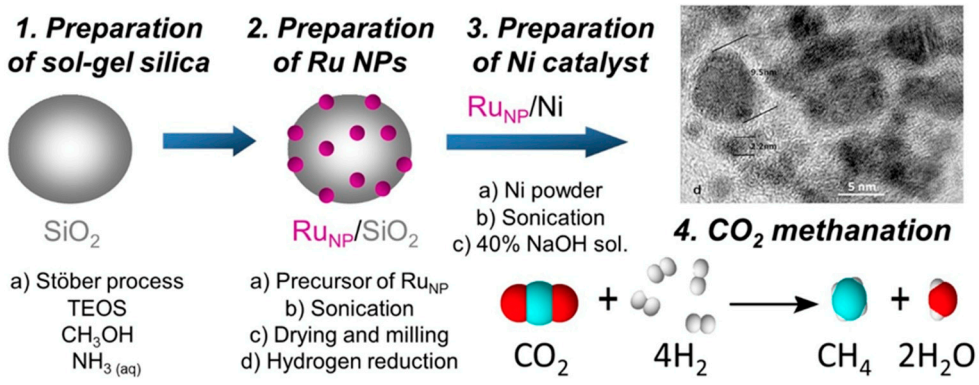

Figure 12. Preparation method of Ru/Ni catalyst for CO_2 methanation. © Adopted from [106].

4. Modeling of the Methanation Catalysis—The Determination of Research Clues

Modelling and simulations in silico are more and more often used in designing and optimizing methanation processes [68,110,111]. In such studies the kinetics of CO_2 methanation is usually modelled by a combination of CO methanation and reversed water-gas shift reaction (RWGSR) [112–114]. The resultant process depends on the rates of both these reactions. The quality of the forecasted model depends on the knowledge of reaction mechanisms and elementary stages, which determine expressions for reaction rates. However, the learning of an exact mechanism and kinetic description is not always unambiguous. This may be explained by varying reaction conditions (e.g., different values of temperatures or partial pressures), the concept of reactor and the applied catalyst, or by assumptions or the

computational method (Langmuir-Hinshelwood, Power Law, elementary reactions, stages of reaction rate) [111]. However, theoretical models are necessary to design catalysts [115]. It was observed that activation energies for elementary surface reactions on catalyst are strongly correlated with adsorption energies, which facilitates identification of significant descriptors [68]. This is illustrated in Figure 13, using the example of CO methanation.

The effect of high dissociation energy is typical of a densely packed surface, while certain surface features (edges, angles, steps, and kinks) enable us to lower the energy barrier [116,117]. Therefore, an active place on the catalyst surface is identified by a convenient nucleation place. The comparison of various metallic surfaces of catalysts (Figure 13a) allows us to state that the activation barrier for CO, CH_4, and H_2O is related to the surface stability of carbon (C) and oxygen (O) forms [68]. The more stable these atoms are, the lower the CO and CH_4 dissociation barrier, and the higher the H_2O formation barrier. It was found that the activation energies also essentially depend linearly on the reaction energy acc. to the so-called Brønsted-Evans-Polanyi relationship (BEP) (Figure 13b) [118]. This enables us to make the rate of reaction on metal surfaces of various catalysts directly dependent on the CO dissociation energy (Figure 13c) [119]. In the case of poor adsorption (right part of graph in Figure 13c), the barrier for product dissociation is high, which limits the reaction rate. For a strong adsorption the rate of removing the adsorbed C and O from the surface is small, hence the barrier for product formation is high. The optimum is situated between these two limits. This effect is a well-known Sabatier rule [120]. In addition, for combinations of different materials, the scaling relationships for the adsorption and energy of transition state of the reaction are unlimited and it becomes possible to optimally adjust the catalysts' activity or selectivity even in the next catalytic sequences [121,122]. Furthermore, this search for catalytic materials is currently supported by machine learning [123]. For example, a sample of a heterogeneous catalyst in a set of different catalysts—catalyst space (defined by composition, carrier type, and particle size) can be described by its features in a certain feature space that is defined by physical properties, atomic properties, and electronic structure. Then machine learning algorithms can generate models or find descriptors that map the features that describe catalysts to their figures of merit (defined by selectivity, activity, and stability). The latest research shows that, thanks to machine learning methods, it is already possible to predict catalytic activity values, reaction descriptors, and potential energy surfaces, and to screen optimal catalysts [123–125].

The designing of catalytic materials with target properties must be described by both the basic (descriptors of anticipated properties) and empirical (measured properties) data. In addition, it is important to gather the data in a structured way, and to consider the possibility of their reorganization and export to any format, so that their processing would be easy and widely available. As a team we have drawn attention to this in the paper "Functional and Material Properties in Nanocatalyst Design: A Data Handling and Sharing Problem" [126], and by creating the "Catalytic Material Database" (CMD), available at cmd.us.edu.pl. The experimental data for heterogeneous catalysts, used mainly in carbon oxides methanation, are gathered in this database. More information on this is available on the database website.

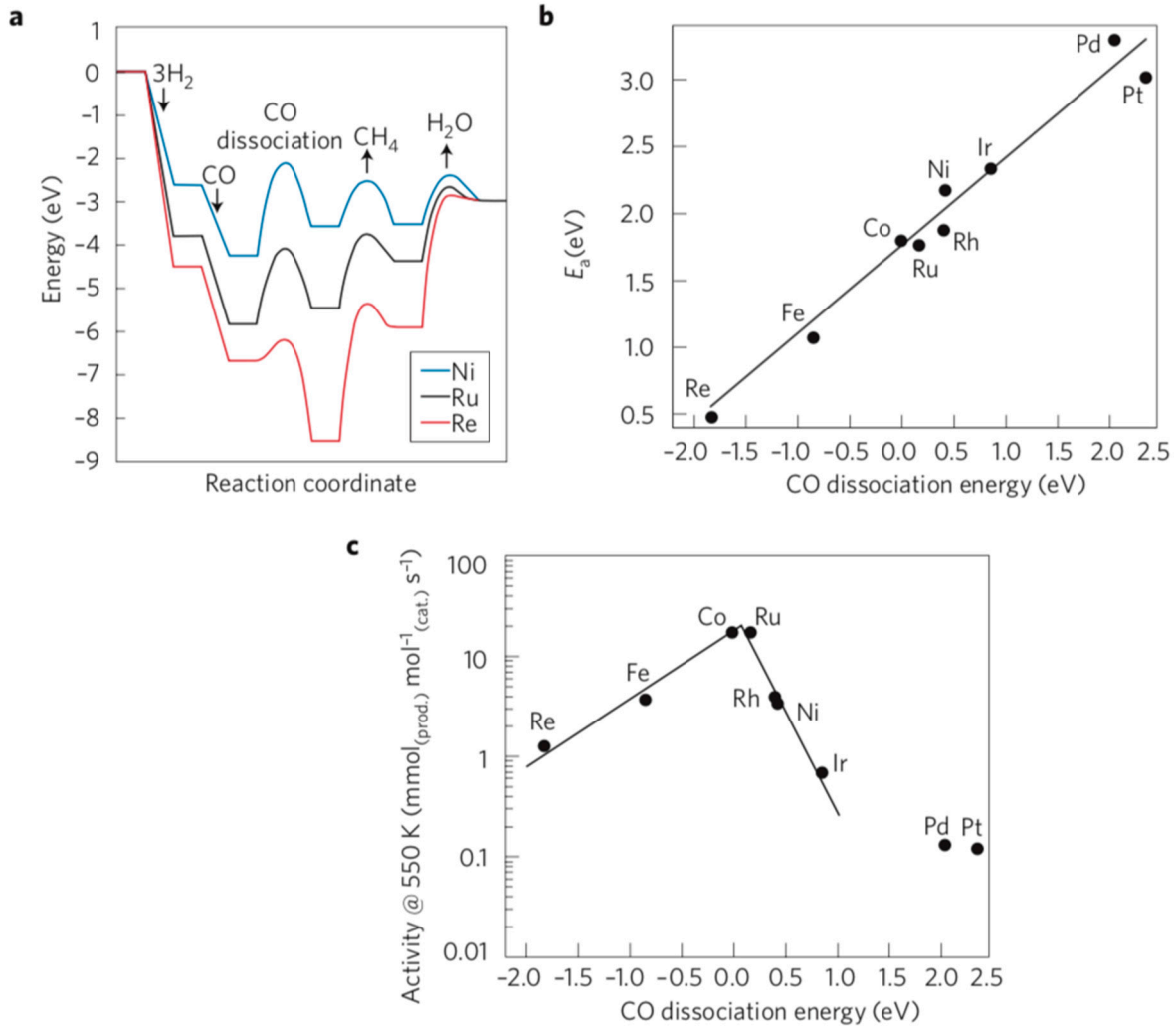

Figure 13. Identification of a descriptor for the CO methanation. © Adopted from [115,119]. (**a**) Calculated energy diagrams for CO methanation over Ni, Ru, and Re. (**b**) Brønsted–Evans–Polanyi relation for CO dissociation over transition metal surfaces. The transition state potential energy, Ea, is linearly related to the CO dissociation energy. (**c**) The corresponding measured volcano-relation for the methanation rate.

Author Contributions: Conceptualization, D.L.; methodology, D.L. and J.P.; validation, D.L., J.P. and M.K.; formal analysis, D.L. and M.K.; investigation, D.L., J.P. and M.K.; resources, J.P.; data curation, D.L., J.P. and M.K.; writing—original draft preparation, D.L. and J.P.; writing—review and editing, D.L., J.P. and M.K.; visualization, D.L. and M.K.; supervision, J.P. and D.L.; project administration, D.L.; funding acquisition, J.P. All authors have read and agreed to the published version of the manuscript.

Funding: This research was funded by National Science Center OPUS 2018/29/B/ST8/02303.

Institutional Review Board Statement: Not applicable.

Informed Consent Statement: Not applicable.

Data Availability Statement: Not applicable.

Acknowledgments: Jaroslaw Polanski would like to acknowledge Zielony Horyzont: New Energy project ZFIN 40001022 for support.

Conflicts of Interest: The authors declare no conflict of interest. The funders had no role in the design of the study; in the collection, analyses, or interpretation of data; in the writing of the manuscript, or in the decision to publish the results.

References

1. CO_2 Annual Mean Data—NOAA Data. Available online: Ftp://aftp.cmdl.noaa.gov/products/trends/co2/co2_annmean_mlo.txt (accessed on 20 August 2021).
2. Brodziński, Z.; Kramarz, M.; Sławomirski, M.R. *Energia Odnawialna Wizytówką Nowoczesnej Gospodarki*; Wydawnictwo Adam Marszałek: Toruń, Poland, 2016; ISBN 978-83-8019-509-7.
3. Smith, M.R.; Myers, S.S. Impact of Anthropogenic CO_2 Emissions on Global Human Nutrition. *Nat. Clim. Chang.* **2018**, *8*, 834–839. [CrossRef]
4. Fletcher, S.E.M. Ocean Circulation Drove Increase in CO_2 Uptake. *Nature* **2017**, *542*, 169–170. [CrossRef] [PubMed]
5. DeVries, T.; Holzer, M.; Primeau, F. Recent Increase in Oceanic Carbon Uptake Driven by Weaker Upper-Ocean Overturning. *Nature* **2017**, *542*, 215–218. [CrossRef] [PubMed]
6. Penuelas, J.; Fernández-Martínez, M.; Vallicrosa, H.; Maspons, J.; Zuccarini, P.; Carnicer, J.; Sanders, T.G.M.; Krüger, I.; Obersteiner, M.; Janssens, I.A.; et al. Increasing Atmospheric CO_2 Concentrations Correlate with Declining Nutritional Status of European Forests. *Commun. Biol.* **2020**, *3*, 125. [CrossRef]
7. European Union Emissions Trading System, EU ETS. Available online: https://ec.europa.eu/clima/policies/ets_en (accessed on 20 August 2021).
8. Pre-2020 Ambition and Implementation-CO_2 Reduction-Kyoto Protocol. Available online: https://unfccc.int/topics/pre-2020 (accessed on 20 August 2021).
9. Kyoto Protocol—Reference Manual. Available online: https://unfccc.int/sites/default/files/08_unfccc_kp_ref_manual.pdf (accessed on 20 August 2020).
10. De Falco, M.D.; Iaquaniello, G.; Centi, G. (Eds.) *CO_2: A Valuable Source of Carbon*, 1st ed.; Green Energy and Technology; Springer: London, UK, 2013; ISBN 978-1-4471-5119-7.
11. 2030 Climate & Energy Framework. Available online: https://ec.europa.eu/clima/policies/strategies/2030_en (accessed on 20 August 2021).
12. Crippa, M.; Oreggioni, G.; Guizzardi, D.; Muntean, M.; Schaaf, E.; Lo Vullo, E.; Solazzo, E.; Monforti-Ferrario, F.; Olivier, J.G.J.; Vignati, E. *Fossil CO_2 and GHG Emissions of All World Countries: 2019 Report*; Publications Office of the European Union: Luxemburg, 2019; ISBN 978-92-76-11100-9.
13. Infografika: Emisje Gazów Cieplarnianych w Unii Europejskiej. Available online: https://www.europarl.europa.eu/news/pl/headlines/society/20180301STO98928/infografika-emisje-gazow-cieplarnianych-w-unii-europejskiej (accessed on 20 August 2021).
14. Global Greenhouse Gas Emissions Data. Available online: https://www.epa.gov/ghgemissions/global-greenhouse-gas-emissions-data (accessed on 20 August 2021).
15. Rozporządzenie Parlamentu Europejskiego i Rady (UE) w Sprawie Wiążących Rocznych Redukcji Emisji Gazów Cieplarnianych. Available online: https://eur-lex.europa.eu/legal-content/PL/TXT/?qid=1582275556293&uri=CELEX:32018R0842 (accessed on 20 August 2021).
16. Quadrelli, E.A.; Centi, G.; Duplan, J.-L.; Perathoner, S. Carbon Dioxide Recycling: Emerging Large-Scale Technologies with Industrial Potential. *ChemSusChem* **2011**, *4*, 1194–1215. [CrossRef]
17. Aresta, M. (Ed.) *Carbon Dioxide as Chemical Feedstock*, 1st ed.; Wiley: Weinheim, Germany, 2010; ISBN 978-3-527-32475-0.
18. Mikkelsen, M.; Jørgensen, M.; Krebs, F.C. The Teraton Challenge. A Review of Fixation and Transformation of Carbon Dioxide. *Energy Environ. Sci.* **2010**, *3*, 43–81. [CrossRef]
19. Peters, M.; Köhler, B.; Kuckshinrichs, W.; Leitner, W.; Markewitz, P.; Müller, T.E. Chemical Technologies for Exploiting and Recycling Carbon Dioxide into the Value Chain. *ChemSusChem* **2011**, *4*, 1216–1240. [CrossRef]
20. Centi, G.; Perathoner, S. Opportunities and Prospects in the Chemical Recycling of Carbon Dioxide to Fuels. *Catal. Today* **2009**, *148*, 191–205. [CrossRef]
21. Dorner, R.W.; Hardy, D.R.; Williams, F.W.; Willauer, H.D. Heterogeneous Catalytic CO_2 Conversion to Value-Added Hydrocarbons. *Energy Environ. Sci.* **2010**, *3*, 884. [CrossRef]
22. International Energy Agency; United Nations Industrial Development Organization. *Carbon Capture and Storage in Industrial Applications*; IEA Technology Roadmaps; OECD: Paris, France, 2012; ISBN 978-92-64-13066-1.
23. Aziz, M.A.A.; Jalil, A.A.; Triwahyono, S.; Ahmad, A. CO_2 Methanation over Heterogeneous Catalysts: Recent Progress and Future Prospects. *Green Chem.* **2015**, *17*, 2647–2663. [CrossRef]
24. Carbon Dioxide Emission by Source Sector (Source: EEA). Available online: https://appsso.eurostat.ec.europa.eu/nui/submitViewTableAction.do (accessed on 20 August 2021).
25. Triantafyllidis, K.S.; Lappas, A.A.; Stöcker, M. (Eds.) *The Role of Catalysis for the Sustainable Production of Bio-Fuels and Bio-Chemicals*, 1st ed.; Elsevier: Amsterdam, The Netherlands; Boston, MA, USA, 2013; ISBN 978-0-444-56330-9.
26. Energy Efficiency and Renewable Energy. *Energy-Intensive Processes Portfolio: Addressing Key Energy Challenges Across U.S. Industry*; Industrial Technologies Program; U.S. Department of Energy: Washington, DC, USA, 2011.
27. Metz, B.; Intergovernmental Panel on Climate Change (Eds.) *IPCC Special Report on Carbon Dioxide Capture and Storage*; Cambridge University Press, for the Intergovernmental Panel on Climate Change: Cambridge, UK, 2005; ISBN 978-0-521-86643-9.
28. Wulf, C.; Linßen, J.; Zapp, P. Review of Power-to-Gas Projects in Europe. *Energy Procedia* **2018**, *155*, 367–378. [CrossRef]

29. Sterner, M. *Bioenergy and Renewable Power Methane in Integrated 100% Renewable Energy Systems: Limiting Global Warming by Transforming Energy Systems*; Erneuerbare Energien und Energieeffizienz/Renewable Energies and Energy Efficiency; Kassel University Press: Kassel, Germany, 2010; ISBN 978-3-89958-798-2.
30. Olah, G.A.; Goeppert, A.; Prakash, G.K.S. *Beyond Oil and Gas: The Methanol Economy*; Wiley-VCH: Weinheim, Germany, 2011; ISBN 978-3-527-64463-6.
31. Grignard, B.; Gennen, S.; Jérôme, C.; Kleij, A.W.; Detrembleur, C. Advances in the Use of CO_2 as a Renewable Feedstock for the Synthesis of Polymers. *Chem. Soc. Rev.* **2019**, *48*, 4466–4514. [CrossRef]
32. Pescarmona, P.P. Cyclic Carbonates Synthesised from CO_2: Applications, Challenges and Recent Research Trends. *Curr. Opin. Green Sustain. Chem.* **2021**, *29*, 100457. [CrossRef]
33. Kelly, M.J.; Barthel, A.; Maheu, C.; Sodpiban, O.; Dega, F.-B.; Vummaleti, S.V.C.; Abou-Hamad, E.; Pelletier, J.D.A.; Cavallo, L.; D'Elia, V.; et al. Conversion of Actual Flue Gas CO_2 via Cycloaddition to Propylene Oxide Catalyzed by a Single-Site, Recyclable Zirconium Catalyst. *J. CO_2 Util.* **2017**, *20*, 243–252. [CrossRef]
34. Sodpiban, O.; Phungpanya, C.; Del Gobbo, S.; Arayachukiat, S.; Piromchart, T.; D'Elia, V. Rational Engineering of Single-Component Heterogeneous Catalysts Based on Abundant Metal Centers for the Mild Conversion of Pure and Impure CO_2 to Cyclic Carbonates. *Chem. Eng. J.* **2021**, *422*, 129930. [CrossRef]
35. Chen, Y.; Luo, R.; Xu, Q.; Jiang, J.; Zhou, X.; Ji, H. Charged Metalloporphyrin Polymers for Cooperative Synthesis of Cyclic Carbonates from CO_2 under Ambient Conditions. *ChemSusChem* **2017**, *10*, 2534–2541. [CrossRef]
36. Fukuoka, S.; Fukawa, I.; Tojo, M.; Oonishi, K.; Hachiya, H.; Aminaka, M.; Hasegawa, K.; Komiya, K. A Novel Non-Phosgene Process for Polycarbonate Production from CO_2: Green and Sustainable Chemistry in Practice. *Catal. Surv. Asia* **2010**, *14*, 146–163. [CrossRef]
37. Demirbas, A.; Demirbas, M.F. *Algae Energy: Algae as a New Source of Biodiesel*; Green Energy and Technology; Springer: Dordrecht, The Netherlands; New York, NY, USA, 2010; ISBN 978-1-84996-050-2.
38. Chiappe, C.; Mezzetta, A.; Pomelli, C.S.; Iaquaniello, G.; Gentile, A.; Masciocchi, B. Development of Cost-Effective Biodiesel from Microalgae Using Protic Ionic Liquids. *Green Chem.* **2016**, *18*, 4982–4989. [CrossRef]
39. Antonovsky, N.; Gleizer, S.; Noor, E.; Zohar, Y.; Herz, E.; Barenholz, U.; Zelcbuch, L.; Amram, S.; Wides, A.; Tepper, N.; et al. Sugar Synthesis from CO_2 in Escherichia Coli. *Cell* **2016**, *166*, 115–125. [CrossRef]
40. Callaway, E.E. Coli Bacteria Engineered to Eat Carbon Dioxide. *Nature* **2019**, *576*, 19–20. [CrossRef]
41. Sharma, T.; Sharma, S.; Kamyab, H.; Kumar, A. Energizing the CO_2 Utilization by Chemo-Enzymatic Approaches and Potentiality of Carbonic Anhydrases: A Review. *J. Clean. Prod.* **2020**, *247*, 119138. [CrossRef]
42. Eckert, C.A.; Knutson, B.L.; Debenedetti, P.G. Supercritical Fluids as Solvents for Chemical and Materials Processing. *Nature* **1996**, *383*, 313–318. [CrossRef]
43. Sodeifian, G.; Sajadian, S.A. Solubility Measurement and Preparation of Nanoparticles of an Anticancer Drug (Letrozole) Using Rapid Expansion of Supercritical Solutions with Solid Cosolvent (RESS-SC). *J. Supercrit. Fluids* **2018**, *133*, 239–252. [CrossRef]
44. Sodeifian, G.; Sajadian, S.A.; Saadati Ardestani, N.; Razmimanesh, F. Production of Loratadine Drug Nanoparticles Using Ultrasonic-Assisted Rapid Expansion of Supercritical Solution into Aqueous Solution (US-RESSAS). *J. Supercrit. Fluids* **2019**, *147*, 241–253. [CrossRef]
45. Sodeifian, G.; Garlapati, C.; Razmimanesh, F.; Ghanaat-Ghamsari, M. Measurement and Modeling of Clemastine Fumarate (Antihistamine Drug) Solubility in Supercritical Carbon Dioxide. *Sci. Rep.* **2021**, *11*, 24344. [CrossRef]
46. Sodeifian, G.; Surya Alwi, R.; Razmimanesh, F.; Abadian, M. Solubility of Dasatinib Monohydrate (Anticancer Drug) in Supercritical CO_2: Experimental and Thermodynamic Modeling. *J. Mol. Liq.* **2022**, *346*, 117899. [CrossRef]
47. Sodeifian, G.; Sajadian, S.A.; Derakhsheshpour, R. CO_2 Utilization as a Supercritical Solvent and Supercritical Antisolvent in Production of Sertraline Hydrochloride Nanoparticles. *J. CO_2 Util.* **2022**, *55*, 101799. [CrossRef]
48. Ameri, A.; Sodeifian, G.; Sajadian, S.A. Lansoprazole Loading of Polymers by Supercritical Carbon Dioxide Impregnation: Impacts of Process Parameters. *J. Supercrit. Fluids* **2020**, *164*, 104892. [CrossRef]
49. Saadati Ardestani, N.; Sodeifian, G.; Sajadian, S.A. Preparation of Phthalocyanine Green Nano Pigment Using Supercritical CO_2 Gas Antisolvent (GAS): Experimental and Modeling. *Heliyon* **2020**, *6*, e04947. [CrossRef]
50. Sodeifian, G.; Saadati Ardestani, N.; Sajadian, S.A.; Soltani Panah, H. Experimental Measurements and Thermodynamic Modeling of Coumarin-7 Solid Solubility in Supercritical Carbon Dioxide: Production of Nanoparticles via RESS Method. *Fluid Phase Equilibria* **2019**, *483*, 122–143. [CrossRef]
51. Sodeifian, G.; Ansari, K. Optimization of Ferulago Angulata Oil Extraction with Supercritical Carbon Dioxide. *J. Supercrit. Fluids* **2011**, *57*, 38–43. [CrossRef]
52. Sodeifian, G.; Saadati Ardestani, N.; Sajadian, S.A.; Ghorbandoost, S. Application of Supercritical Carbon Dioxide to Extract Essential Oil from Cleome Coluteoides Boiss: Experimental, Response Surface and Grey Wolf Optimization Methodology. *J. Supercrit. Fluids* **2016**, *114*, 55–63. [CrossRef]
53. White, M.T.; Bianchi, G.; Chai, L.; Tassou, S.A.; Sayma, A.I. Review of Supercritical CO_2 Technologies and Systems for Power Generation. *Appl. Therm. Eng.* **2021**, *185*, 116447. [CrossRef]
54. Climeworks-CO_2 Removal. Available online: https://climeworks.com (accessed on 23 August 2021).
55. Ghiasi, M.; Zeinali, P.; Gholami, S.; Zahedi, M. Separation of CH_4, H_2S, N_2 and CO_2 Gases Using Four Types of Nanoporous Graphene Cluster Model: A Quantum Chemical Investigation. *J. Mol. Model.* **2021**, *27*, 201. [CrossRef]

56. Shaikh, A.R.; Ashraf, M.; AlMayef, T.; Chawla, M.; Poater, A.; Cavallo, L. Amino Acid Ionic Liquids as Potential Candidates for CO_2 Capture: Combined Density Functional Theory and Molecular Dynamics Simulations. *Chem. Phys. Lett.* **2020**, *745*, 137239. [CrossRef]
57. Sabatier, P.; Senderens, J.-B. Nouvelles Synthèses Du Méthane. *Comptes Rendus l'Académie Sci.* **1902**, *134*, 514–516.
58. Barbarossa, V.; Vanga, G. *Energia, Ambiente e Innovazione*; ENEA: Rome, Italy, 2011; pp. 82–85.
59. Gao, J.; Liu, Q.; Gu, F.; Liu, B.; Zhong, Z.; Su, F. Recent Advances in Methanation Catalysts for the Production of Synthetic Natural Gas. *RSC Adv.* **2015**, *5*, 22759–22776. [CrossRef]
60. Artz, J.; Müller, T.E.; Thenert, K.; Kleinekorte, J.; Meys, R.; Sternberg, A.; Bardow, A.; Leitner, W. Sustainable Conversion of Carbon Dioxide: An Integrated Review of Catalysis and Life Cycle Assessment. *Chem. Rev.* **2018**, *118*, 434–504. [CrossRef]
61. Centi, G.; Perathoner, S. Heterogeneous Catalytic Reactions with CO_2: Status and Perspectives. In *Studies in Surface Science and Catalysis*; Elsevier: Amsterdam, The Netherlands, 2004; Volume 153, pp. 1–8, ISBN 978-0-444-51600-8.
62. Jessop, P.G.; Joó, F.; Tai, C.-C. Recent Advances in the Homogeneous Hydrogenation of Carbon Dioxide. *Coord. Chem. Rev.* **2004**, *248*, 2425–2442. [CrossRef]
63. Rönsch, S.; Schneider, J.; Matthischke, S.; Schlüter, M.; Götz, M.; Lefebvre, J.; Prabhakaran, P.; Bajohr, S. Review on Methanation—From Fundamentals to Current Projects. *Fuel* **2016**, *166*, 276–296. [CrossRef]
64. Choe, S.J.; Kang, H.-J.; Kim, S.-J.; Park, S.-B.; Park, D.H.; Huh, D.S. Adsorbed Carbon Formation and Carbon Hydrogenation for CO_2 Methanation on the Ni(111) Surface: ASED-MO Study. *Bull. Korean Chem. Soc.* **2005**, *26*, 1682–1688. [CrossRef]
65. Hwang, S.; Lee, J.; Hong, U.G.; Seo, J.G.; Jung, J.C.; Koh, D.J.; Lim, H.; Byun, C.; Song, I.K. Methane Production from Carbon Monoxide and Hydrogen over Nickel–Alumina Xerogel Catalyst: Effect of Nickel Content. *J. Ind. Eng. Chem.* **2011**, *17*, 154–157. [CrossRef]
66. Tada, S.; Ikeda, S.; Shimoda, N.; Honma, T.; Takahashi, M.; Nariyuki, A.; Satokawa, S. Sponge Ni Catalyst with High Activity in CO_2 Methanation. *Int. J. Hydrogen Energy* **2017**, *42*, 30126–30134. [CrossRef]
67. Polanski, J.; Lach, D.; Kapkowski, M.; Bartczak, P.; Siudyga, T.; Smolinski, A. Ru and Ni—Privileged Metal Combination for Environmental Nanocatalysis. *Catalysts* **2020**, *10*, 992. [CrossRef]
68. Bligaard, T.; Nørskov, J.K.; Dahl, S.; Matthiesen, J.; Christensen, C.H.; Sehested, J. The Brønsted–Evans–Polanyi Relation and the Volcano Curve in Heterogeneous Catalysis. *J. Catal.* **2004**, *224*, 206–217. [CrossRef]
69. Kai, T.; Yamasaki, Y.; Takahashi, T.; Masumoto, T.; Kimura, H. Increase in the Thermal Stability during the Methanation of CO_2 over a Rh Catalyst Prepared from an Amorphous Alloy. *Can. J. Chem. Eng.* **1998**, *76*, 331–335. [CrossRef]
70. Martin, N.M.; Hemmingsson, F.; Wang, X.; Merte, L.R.; Hejral, U.; Gustafson, J.; Skoglundh, M.; Meira, D.M.; Dippel, A.-C.; Gutowski, O.; et al. Structure–Function Relationship during CO_2 Methanation over Rh/Al_2O_3 and Rh/SiO_2 Catalysts under Atmospheric Pressure Conditions. *Catal. Sci. Technol.* **2018**, *8*, 2686–2696. [CrossRef]
71. Benítez, J.J.; Alvero, R.; Capitán, M.J.; Carrizosa, I.; Odriozola, J.A. DRIFTS Study of Adsorbed Formate Species in the Carbon Dioxide and Hydrogen Reaction over Rhodium Catalysts. *Appl. Catal.* **1991**, *71*, 219–231. [CrossRef]
72. Abe, T.; Tanizawa, M.; Watanabe, K.; Taguchi, A. CO_2 Methanation Property of Ru Nanoparticle-Loaded TiO_2 Prepared by a Polygonal Barrel-Sputtering Method. *Energy Environ. Sci.* **2009**, *2*, 315. [CrossRef]
73. Siudyga, T.; Kapkowski, M.; Janas, D.; Wasiak, T.; Sitko, R.; Zubko, M.; Szade, J.; Balin, K.; Klimontko, J.; Lach, D.; et al. Nano-Ru Supported on Ni Nanowires for Low-Temperature Carbon Dioxide Methanation. *Catalysts* **2020**, *10*, 513. [CrossRef]
74. Snytnikov, P.V.; Zyryanova, M.M.; Sobyanin, V.A. CO-Cleanup of Hydrogen-Rich Stream for LT PEM FC Feeding: Catalysts and Their Performance in Selective CO Methanation. *Top. Catal.* **2016**, *59*, 1394–1412. [CrossRef]
75. Ross, J.R.H. *Contemporary Catalysis: Fundamentals and Current Applications*; Elsevier: Amsterdam, The Netherlands, 2019; ISBN 978-0-444-63474-0.
76. Martínez, J.; Hernández, E.; Alfaro, S.; López Medina, R.; Valverde Aguilar, G.; Albiter, E.; Valenzuela, M. High Selectivity and Stability of Nickel Catalysts for CO_2 Methanation: Support Effects. *Catalysts* **2018**, *9*, 24. [CrossRef]
77. Le, T.A.; Kim, M.S.; Lee, S.H.; Kim, T.W.; Park, E.D. CO and CO_2 Methanation over Supported Ni Catalysts. *Catal. Today* **2017**, *293–294*, 89–96. [CrossRef]
78. Fan, M.-T.; Miao, K.-P.; Lin, J.-D.; Zhang, H.-B.; Liao, D.-W. Mg-Al Oxide Supported Ni Catalysts with Enhanced Stability for Efficient Synthetic Natural Gas from Syngas. *Appl. Surf. Sci.* **2014**, *307*, 682–688. [CrossRef]
79. Hu, D.; Gao, J.; Ping, Y.; Jia, L.; Gunawan, P.; Zhong, Z.; Xu, G.; Gu, F.; Su, F. Enhanced Investigation of CO Methanation over Ni/Al_2O_3 Catalysts for Synthetic Natural Gas Production. *Ind. Eng. Chem. Res.* **2012**, *51*, 4875–4886. [CrossRef]
80. Qin, H.; Guo, C.; Wu, Y.; Zhang, J. Effect of La_2O_3 Promoter on NiO/Al_2O_3 Catalyst in CO Methanation. *Korean J. Chem. Eng.* **2014**, *31*, 1168–1173. [CrossRef]
81. Liu, Q.; Gu, F.; Lu, X.; Liu, Y.; Li, H.; Zhong, Z.; Xu, G.; Su, F. Enhanced Catalytic Performances of Ni/Al_2O_3 Catalyst via Addition of V_2O_3 for CO Methanation. *Appl. Catal. A-Gen.* **2014**, *488*, 37–47. [CrossRef]
82. Liu, H.; Zou, X.; Wang, X.; Lu, X.; Ding, W. Effect of CeO_2 Addition on Ni/Al_2O_3 Catalysts for Methanation of Carbon Dioxide with Hydrogen. *J. Nat. Gas Chem.* **2012**, *21*, 703–707. [CrossRef]
83. Campbell, C.T.; Goodman, D.W. A Surface Science Investigation of the Role of Potassium Promoters in Nickel Catalysts for CO Hydrogenation. *Surf. Sci.* **1982**, *123*, 413–426. [CrossRef]

84. Aldana, P.A.U.; Ocampo, F.; Kobl, K.; Louis, B.; Thibault-Starzyk, F.; Daturi, M.; Bazin, P.; Thomas, S.; Roger, A.C. Catalytic CO_2 Valorization into CH_4 on Ni-Based Ceria-Zirconia. Reaction Mechanism by Operando IR Spectroscopy. *Catal. Today* **2013**, *215*, 201–207. [CrossRef]
85. Pan, Q.; Peng, J.; Wang, S.; Wang, S. In Situ FTIR Spectroscopic Study of the CO_2 Methanation Mechanism on $Ni/Ce_{0.5}Zr_{0.5}O_2$. *Catal. Sci. Technol.* **2014**, *4*, 502–509. [CrossRef]
86. Fujita, S.; Nakamura, M.; Doi, T.; Takezawa, N. Mechanisms of Methanation of Carbon Dioxide and Carbon Monoxide over Nickel/Alumina Catalysts. *Appl. Catal. A-Gen.* **1993**, *104*, 87–100. [CrossRef]
87. Karelovic, A.; Ruiz, P. Improving the Hydrogenation Function of Pd/γ-Al_2O_3 Catalyst by Rh/γ-Al_2O_3 Addition in CO_2 Methanation at Low Temperature. *ACS Catal.* **2013**, *3*, 2799–2812. [CrossRef]
88. Aziz, M.A.A.; Jalil, A.A.; Triwahyono, S.; Sidik, S.M. Methanation of Carbon Dioxide on Metal-Promoted Mesostructured Silica Nanoparticles. *Appl. Catal. A-Gen.* **2014**, *486*, 115–122. [CrossRef]
89. Aziz, M.A.A.; Jalil, A.A.; Triwahyono, S.; Mukti, R.R.; Taufiq-Yap, Y.H.; Sazegar, M.R. Highly Active Ni-Promoted Mesostructured Silica Nanoparticles for CO_2 Methanation. *Appl. Catal. B* **2014**, *147*, 359–368. [CrossRef]
90. Aziz, M.A.A.; Jalil, A.A.; Triwahyono, S.; Saad, M.W.A. CO_2 Methanation over Ni-Promoted Mesostructured Silica Nanoparticles: Influence of Ni Loading and Water Vapor on Activity and Response Surface Methodology Studies. *Chem. Eng. J.* **2015**, *260*, 757–764. [CrossRef]
91. Kärger, J.; Ruthven, D.M.; Theodorou, D.N. *Diffusion in Nanoporous Materials*, 1st ed.; Wiley: Hoboken, NJ, USA, 2012; ISBN 978-3-527-31024-1.
92. Kärger, J.; Goepel, M.; Gläser, R. Diffusion in Nanocatalysis. In *Nanotechnology in Catalysis*; Van de Voorde, M., Sels, B., Eds.; Wiley-VCH Verlag GmbH & Co. KGaA: Weinheim, Germany, 2017; pp. 293–334, ISBN 978-3-527-69982-7.
93. Tesser, R.; Santacesaria, E. Revisiting the Role of Mass and Heat Transfer in Gas–Solid Catalytic Reactions. *Processes* **2020**, *8*, 1599. [CrossRef]
94. Dai, X.; Sun, Y. Reduction of Carbon Dioxide on Photoexcited Nanoparticles of VIII Group Metals. *Nanoscale* **2019**, *11*, 16723–16732. [CrossRef]
95. Robatjazi, H.; Zhao, H.; Swearer, D.F.; Hogan, N.J.; Zhou, L.; Alabastri, A.; McClain, M.J.; Nordlander, P.; Halas, N.J. Plasmon-Induced Selective Carbon Dioxide Conversion on Earth-Abundant Aluminum-Cuprous Oxide Antenna-Reactor Nanoparticles. *Nat. Commun.* **2017**, *8*, 27. [CrossRef]
96. Kale, M.J.; Avanesian, T.; Xin, H.; Yan, J.; Christopher, P. Controlling Catalytic Selectivity on Metal Nanoparticles by Direct Photoexcitation of Adsorbate–Metal Bonds. *Nano Lett.* **2014**, *14*, 5405–5412. [CrossRef]
97. Kim, Y.; Dumett Torres, D.; Jain, P.K. Activation Energies of Plasmonic Catalysts. *Nano Lett.* **2016**, *16*, 3399–3407. [CrossRef]
98. Pinchuk, A.; von Plessen, G.; Kreibig, U. Influence of Interband Electronic Transitions on the Optical Absorption in Metallic Nanoparticles. *J. Phys. D Appl. Phys.* **2004**, *37*, 3133–3139. [CrossRef]
99. Pinchuk, A.; Kreibig, U.; Hilger, A. Optical Properties of Metallic Nanoparticles: Influence of Interface Effects and Interband Transitions. *Surf. Sci.* **2004**, *557*, 269–280. [CrossRef]
100. Zhang, C.; Kong, T.; Fu, Z.; Zhang, Z.; Zheng, H. Hot Electron and Thermal Effects in Plasmonic Catalysis of Nanocrystal Transformation. *Nanoscale* **2020**, *12*, 8768–8774. [CrossRef] [PubMed]
101. Kim, C.; Hyeon, S.; Lee, J.; Kim, W.D.; Lee, D.C.; Kim, J.; Lee, H. Energy-Efficient CO_2 Hydrogenation with Fast Response Using Photoexcitation of CO_2 Adsorbed on Metal Catalysts. *Nat. Commun.* **2018**, *9*, 3027. [CrossRef] [PubMed]
102. Schwarz, J.A.; Contescu, C.; Contescu, A. Methods for Preparation of Catalytic Materials. *Chem. Rev.* **1995**, *95*, 477–510. [CrossRef]
103. Stöber, W.; Fink, A.; Bohn, E. Controlled Growth of Monodisperse Silica Spheres in the Micron Size Range. *J. Colloid Interface Sci.* **1968**, *26*, 62–69. [CrossRef]
104. Rao, K.S.; El-Hami, K.; Kodaki, T.; Matsushige, K.; Makino, K. A Novel Method for Synthesis of Silica Nanoparticles. *J. Colloid Interface Sci.* **2005**, *289*, 125–131. [CrossRef]
105. Polanski, J.; Bartczak, P.; Ambrozkiewicz, W.; Sitko, R.; Siudyga, T.; Mianowski, A.; Szade, J.; Balin, K.; Lelątko, J. Ni-Supported Pd Nanoparticles with Ca Promoter: A New Catalyst for Low-Temperature Ammonia Cracking. *PLoS ONE* **2015**, *10*, e0136805. [CrossRef]
106. Polanski, J.; Siudyga, T.; Bartczak, P.; Kapkowski, M.; Ambrozkiewicz, W.; Nobis, A.; Sitko, R.; Klimontko, J.; Szade, J.; Lelątko, J. Oxide Passivated Ni-Supported Ru Nanoparticles in Silica: A New Catalyst for Low-Temperature Carbon Dioxide Methanation. *Appl. Catal. B.* **2017**, *206*, 16–23. [CrossRef]
107. Siudyga, T.; Kapkowski, M.; Bartczak, P.; Zubko, M.; Szade, J.; Balin, K.; Antoniotti, S.; Polanski, J. Ultra-Low Temperature Carbon (Di)Oxide Hydrogenation Catalyzed by Hybrid Ruthenium–Nickel Nanocatalysts: Towards Sustainable Methane Production. *Green Chem.* **2020**, *22*, 5143–5150. [CrossRef]
108. Kapkowski, M.; Bartczak, P.; Korzec, M.; Sitko, R.; Szade, J.; Balin, K.; Lelątko, J.; Polanski, J. SiO_2-, Cu-, and Ni-Supported Au Nanoparticles for Selective Glycerol Oxidation in the Liquid Phase. *J. Catal.* **2014**, *319*, 110–118. [CrossRef]
109. Korzec, M.; Bartczak, P.; Niemczyk, A.; Szade, J.; Kapkowski, M.; Zenderowska, P.; Balin, K.; Lelątko, J.; Polanski, J. Bimetallic Nano-Pd/PdO/Cu System as a Highly Effective Catalyst for the Sonogashira Reaction. *J. Catal.* **2014**, *313*, 1–8. [CrossRef]
110. Rönsch, S.; Köchermann, J.; Schneider, J.; Matthischke, S. Global Reaction Kinetics of CO and CO_2 Methanation for Dynamic Process Modeling. *Chem. Eng. Technol.* **2016**, *39*, 208–218. [CrossRef]

111. Hernandez Lalinde, J.A.; Roongruangsree, P.; Ilsemann, J.; Bäumer, M.; Kopyscinski, J. CO_2 Methanation and Reverse Water Gas Shift Reaction. Kinetic Study Based on in Situ Spatially-Resolved Measurements. *Chem. Eng. J.* **2020**, *390*, 124629. [CrossRef]
112. Kopyscinski, J.; Schildhauer, T.J.; Biollaz, S.M.A. Methanation in a Fluidized Bed Reactor with High Initial CO Partial Pressure: Part II— Modeling and Sensitivity Study. *Chem. Eng. Sci.* **2011**, *66*, 1612–1621. [CrossRef]
113. Champon, I.; Bengaouer, A.; Chaise, A.; Thomas, S.; Roger, A.-C. Carbon Dioxide Methanation Kinetic Model on a Commercial Ni/Al_2O_3 Catalyst. *J. CO_2 Util.* **2019**, *34*, 256–265. [CrossRef]
114. Xu, J.; Froment, G.F. Methane Steam Reforming, Methanation and Water-Gas Shift: I. Intrinsic Kinetics. *AIChE J.* **1989**, *35*, 88–96. [CrossRef]
115. Nørskov, J.K.; Bligaard, T.; Rossmeisl, J.; Christensen, C.H. Towards the Computational Design of Solid Catalysts. *Nat. Chem.* **2009**, *1*, 37–46. [CrossRef]
116. Nørskov, J.K.; Bligaard, T.; Logadottir, A.; Bahn, S.; Hansen, L.B.; Bollinger, M.; Bengaard, H.; Hammer, B.; Sljivancanin, Z.; Mavrikakis, M.; et al. Universality in Heterogeneous Catalysis. *J. Catal.* **2002**, *209*, 275–278. [CrossRef]
117. Ciobica, I.M.; van Santen, R.A. Carbon Monoxide Dissociation on Planar and Stepped Ru(0001) Surfaces. *J. Phys. Chem. B* **2003**, *107*, 3808–3812. [CrossRef]
118. Michaelides, A.; Liu, Z.-P.; Zhang, C.J.; Alavi, A.; King, D.A.; Hu, P. Identification of General Linear Relationships between Activation Energies and Enthalpy Changes for Dissociation Reactions at Surfaces. *J. Am. Chem. Soc.* **2003**, *125*, 3704–3705. [CrossRef]
119. Andersson, M.; Bligaard, T.; Kustov, A.; Larsen, K.; Greeley, J.; Johannessen, T.; Christensen, C.; Norskov, J. Toward Computational Screening in Heterogeneous Catalysis: Pareto-Optimal Methanation Catalysts. *J. Catal.* **2006**, *239*, 501–506. [CrossRef]
120. Sabatier, P. Hydrogénations et déshydrogénations par catalyse. *Ber. Dtsch. Chem. Ges.* **1911**, *44*, 1984–2001. [CrossRef]
121. Kumar, G.; Nikolla, E.; Linic, S.; Medlin, J.W.; Janik, M.J. Multicomponent Catalysts: Limitations and Prospects. *ACS Catal.* **2018**, *8*, 3202–3208. [CrossRef]
122. Greeley, J. Theoretical Heterogeneous Catalysis: Scaling Relationships and Computational Catalyst Design. *Annu. Rev. Chem. Biomol. Eng.* **2016**, *7*, 605–635. [CrossRef]
123. Goldsmith, B.R.; Esterhuizen, J.; Liu, J.; Bartel, C.J.; Sutton, C. Machine Learning for Heterogeneous Catalyst Design and Discovery. *AIChE J.* **2018**, *64*, 2311–2323. [CrossRef]
124. Suzuki, K.; Toyao, T.; Maeno, Z.; Takakusagi, S.; Shimizu, K.; Takigawa, I. Statistical Analysis and Discovery of Heterogeneous Catalysts Based on Machine Learning from Diverse Published Data. *ChemCatChem* **2019**, *11*, 4537–4547. [CrossRef]
125. Ouyang, R.; Xie, Y.; Jiang, D. Global Minimization of Gold Clusters by Combining Neural Network Potentials and the Basin-Hopping Method. *Nanoscale* **2015**, *7*, 14817–14821. [CrossRef]
126. Lach, D.; Zhdan, U.; Smolinski, A.; Polanski, J. Functional and Material Properties in Nanocatalyst Design: A Data Handling and Sharing Problem. *IJMS* **2021**, *22*, 5176. [CrossRef]